Biomaterials Science

Development of a Microdevice-based Human Mesenchymal Stem Cell-mediated Drug Delivery System

Journal:	*Biomaterials Science*
Manuscript ID	BM-ART-12-2018-001634.R1
Article Type:	Paper
Date Submitted by the Author:	02-Mar-2019
Complete List of Authors:	Xia, Junfei; Florida A&M University-Florida State University College of Engineering, Chemical and Biomedical Engineering Tsai, Ang Chen; Florida A&M University-Florida State University College of Engineering, Chemical and Biomedical Engineering Cheng, Wenhao; Florida A&M University-Florida State University College of Engineering, Chemical and Biomedical Engineering Yuan, Xuegang; Florida A&M University-Florida State University College of Engineering, Chemical and Biomedical Engineering Ma, Teng; Florida State University, Chemical and Biomedical Engineering Guan, Jingjiao; Florida State University, Department of Chemical and Biomedical Engineering

Development of a Microdevice-based Human Mesenchymal Stem Cell-mediated Drug Delivery System

Junfei Xia, Ang Chen Tsai, Wenhao Cheng, Xuegang Yuan, Teng Ma, Jingjiao Guan*

Department of Chemical and Biomedical Engineering
Florida A&M University-Florida State University College of Engineering
2525 Pottsdamer Street
Tallahassee, Florida 32310-2870, USA

* Corresponding author
Tel.: 18504106643
E-mail address: guan@eng.famu.fsu.edu

Abstract

Cell-mediated drug delivery systems utilize living cells as vehicles to achieve controlled delivery of drugs. One of the systems features integrating cells with disk-shaped microparticles termed microdevices into cell-microdevice complexes that possess some unique advantages over its counterparts. Human mesenchymal stem cells (hMSCs) have been extensively studied as therapeutic cells and used as carrier cells for drug-loaded nanoparticles or other functional nanoparticles. This article presents development of a microdevice-based hMSC-mediated drug delivery system for the first time. This study revealed that the microdevices could be attached to the hMSCs in a controlled and versatile manner; the produced hMSC-microdevice complexes were stable over cultivation and trypsinization; and the microdevice attachment did not affect the viability and proliferation of the hMSCs. Moreover, cultured microdevice-bound hMSCs retained their abilities to migrate on a flat surface, form a spheroid, and actively dissociate from the spheroid. These results indicate that this microdevice-based hMSC-mediated system promises to be further developed into a clinically viable drug delivery system.

Keywords: drug delivery, mesenchymal stem cell, spheroid, microparticle, microdevice

1. Introduction

Cell-mediated drug delivery systems feature the use of living cells to deliver exogenous therapeutic agents for treating human diseases. This strategy allows harnessing unique cellular capabilities that are unattainable by nonliving vehicles to achieve highly controlled drug delivery. The cargo agents of these systems are dominantly in the form of nanoparticles, which are synthesized by a bottom-up approach, either loaded inside the carrier cells or attached to their outer surface [1,2]. Compared to the nanoparticles, microparticles fabricated by a top-down approach possess some advantages for this application such as a better control of the particle geometry, structure and composition, and particle-cell interaction [3,4,5,6,7,8]. Specifically, Rubner's group developed microparticles termed cellular backpacks, which were fabricated with photolithography and layer-by-layer assembly (LbL) [3]. The "backpacks" not only had highly uniform shape and size, and a multilayered structure, but also could resist phagocytosis by macrophages. Furthermore, Batrakova's group successfully used the "backpacks" to deliver catalase across the blood-brain barrier in mice with monocytes/macrophages as the carrier cells [4]. Our group integrated soft lithography with several film-deposition techniques such as spin coating and LbL to produce microparticles referred to as microdevices with a variety of materials [5,6,7,8]. Moreover, we developed a simple method for producing cell-microdevice complexes [9]. This method, which was based on firstly seeding cells on microdevices printed on a temperature-sensitive sacrificial layer at the room temperature and then releasing the cell-microdevice complexes by raising the temperature, was also used in this study.

Central to any cell-mediated drug system is the carrier cell. Recently, human mesenchymal stem cells (hMSCs) become a primary candidate for clinical cell therapy due to its ease of access, lack of ethnic concerns, low immunogenicity, multilineage differentiation potential, ability to home to injury sites, anti-inflammation character, capability to produce trophic factors, and plasticity for genetic engineering [10,11,12]. Moreover, hMSCs have been utilized as the carrier cells in cell-mediated drug delivery systems especially for tumoritropic drug delivery [13,14,15,16]. Specifically, Cheng *et al.* attached nanoparticles to the surface of hMSCs and found the nanoparticle-bound cells retained their inherent tumoritropic properties *in vitro* [13]. Roger *et al.* injected hMSCs that internalized drug-loaded nanoparticles into a tumor site in a mouse model and found the cells could migrate toward the tumor [14]. Li *et al.* attached drug-loaded silica nanoparticles to hMSCs and demonstrated that the system enhanced delivery of the drug to a model tumor in a mouse [15]. Sadhukha *et al.* later reported that hMSCs carrying drug-loaded nanoparticles accumulated in lung tumors in mice following an intravenous injection [16]. We previously attached microdevices to the surface of a hMSC spheroid, but have never produced hMSC-microdevice complexes composed of individual hMSCs [9]. Since individual hMSCs are the structural and functional units of a typical hMSC-mediated drug delivery system, here we report the development of a system based on individual hMSCs attached by microdevices for the first time. Specifically, this study covers production and stability of hMSC-microdevice complexes, and effects of the microdevice attachment on the viability, proliferation and migration of the hMSCs and capability of the hMSCs to form a spheroid and dissociate from

it. The ultimate goal of this research is to develop a clinically viable hMSC-mediated drug delivery system that unifies the unique strengths of the microdevices and hMSCs for treating solid tumors.

2. Materials and methods

2.1. Materials

Acid-terminated poly(D,L-lactic-co-glycolic) acid (PLGA) with a lactide-to-glycolide ratio of 75:25 and a molecular weight (MW) of 4-15 kDa, poly(allylamine hydrochloride) (PAH) with a MW of 58 kDa, poly(sodium 4-styrenesulfonate) (PSS) with a MW of 100 kDa, poly(N-isopropylacrylamide) (PNIPAM) with a MW of 10-15 kDa, 1H,1H,2H,2H-perfluorooctyltriethoxysilane, thiazolyl blue tetrazolium bromide (MTT), 3,3'–dioctadecyloxacarbocyanine perchlorate (DiO) were purchased from Sigma-Aldrich (St. Louis, Missouri). Poly(propyl methacrylate) (PPMA) was purchased from Scientific Polymer Products Inc (Ontario, New York). Octadecyl rhodamine B chloride (R18) was purchased from Biotium (Fremont, California). Hoechst 33342 was purchased from Life Technologies. Poly-L-lysine hydrobromide (PLL) with a MW of 30-70 kDa was purchased from MP Biomedicals LLC (Santa Ana, California). Human serum albumin (HSA), calcein AM and proteinase K were purchased from VWR (Radnor, Pennsylvania). Alexa Fluor™ 594 phalloidin, minimum essential medium-alpha (α-MEM), Penicillin/Streptomycin were purchased from ThermoFisher (Waltham, Massachusetts). Sylgard 184 poly(dimethyl siloxane) (PDMS) kit was purchased from Dow Corning (Midland, Michigan). Fetal bovine serum (FBS) was purchased from Atlanta Biologicals (Lawrenceville, Georgia). PicoGreen was purchased from Molecular Probes (Eugene, Oregon).

2.2. Preparation of PNIPAM-coated glass slides

Glass slides were cleaned with oxygen plasma (PDC-32G plasma cleaner, Harrick Plasma, Ithaca, New York). The slides were placed in a vacuum desiccator with ~100 μL trichloro (1H,1H,2H,2H-perfluorooctyl) silane in a centrifuge tube. A vacuum pump was used to create a low pressure in the desiccator. The desiccator was placed in a 65 °C oven. After 12 h, the slides were taken out, washed with water, and dried under a stream of nitrogen. A solution of PNIPAM in ethanol (2 wt%) was spin-coated on the slides (500 revolutions per minute (rpm), 1 min). The slides were then placed in a desiccator. After a low pressure was created in the desiccator as described above, the desiccator was placed in a 65 °C oven and kept for 2 h.

2.3. Fabrication of microdevices

The fabrication procedure is schematically shown in Fig. 1. PDMS stamps carrying an array of pillars with a diameter of 10 μm, a height of 8 μm, and a center-to-center distance of 30 μm in the hexagonal lattice were used throughout this study unless otherwise noted. Microdevices with two different compositions were fabricated in this study. One was termed as

PAH/PSS/PAH/PPMA(R18 or DiO), meaning that PAH was the first layer deposited on the stamp, followed by a layer of PSS, another layer of PAH, and finally a layer of PPMA containing R18 or DiO. The other type of microdevices was termed as PLL-FITC/HSA/PLL/PLGA(R18), where PLL-FITC represents PLL conjugated with FITC. To produce the PAH/PSS/PAH/PPMA(R18 or DiO) microdevices, a stamp was firstly soaked in an aqueous PAH solution (1 wt%, pH 10) for 15 min, followed by a water wash. This step was repeated with an aqueous PSS solution (1 wt%, pH 5.8) and the PAH solution sequentially. The stamp was then dried under a stream of nitrogen. Next, PPMA was spin-coated onto the stamp using a solution of PPMA in acetone (200 μL, 4 wt%, 10 μg/mL R18 or DiO) at 2,000 rpm for 1 min. The stamp was then brought into contact with a PNIPAM-coated glass slide on a hot plate at 110 °C. After 5 s, the slide and stamp were transferred together from the hot stage onto a table surface at the room temperature. After 30 s, the stamp was peeled off from the slide. A slightly different procedure was used to produce the PAH/PSS/PAH/PPMA(R18) microdevices with a stamp carrying an array of circular pillars with a diameter of 7 μm, a height of 3.4 μm, and a center-to-center distance of 20 μm in the square lattice. The procedure is as follows. PNIPAM in ethanol (2 wt%, 220 μL) was added into a well of a standard 12-well plate for tissue culture. The plate was kept at room temperature for 12 h and then in a 65 °C oven for 12 h. The trilayer of PAH/PSS/PAH was deposited on the stamp as above. PPMA was then spin-coated onto the stamp using a solution of PPMA in acetone (5 wt%, 50 μg/mL R18) at a spin rate of 3,000 rpm for 1 min. Next, the stamp was brought into contact with the PNIPAM-coated floor of the well. After 3 s, the stamp was peeled off. To produce the PLL-FITC/HSA/PLL/PLGA (R18) microdevices, a stamp was firstly soaked in an aqueous PLL-FITC solution (0.1 wt%, pH 10) for 30 min, followed by a water wash. This step was repeated with an aqueous HSA solution (1 mg/mL, pH 7) and an aqueous PLL solution (0.1 wt%, pH 5.8) sequentially. The stamp was then dried under a stream of nitrogen. Next, PLGA was spin-coated onto the stamp using a solution of PLGA in acetone (200 μL, 12 wt%, 10 μg/mL R18) at 2,000 rpm for 1 min. The stamp was then brought into contact with a PNIPAM-coated glass slide on a hot plate at 50 °C. After 5 s, the slide and stamp were transferred together from the hot stage onto a table surface at the room temperature. After 30 s, the stamp was peeled off from the slide.

2.4. Cell culture

Frozen hMSCs at passage 1 were obtained from the Tulane Center for Stem Cell Research and Regenerative Medicine [17]. hMSCs were isolated from the human bone marrow of healthy donors ranging in age from 19 to 49 years based on plastic adherence, being negative for CD34, CD45, CD117 (all less than 2%) and positive for CD29, CD44, CD49c, CD90, CD105 and CD147 markers (greater than 95%), and possessing tri-lineage differentiation potential upon induction *in vitro*. Frozen hMSCs in liquid nitrogen were thawed and expanded on 150-mm tissue culture petri dishes (Corning, Corning, New York) at a density of approximately 1,500 cells/cm^2 with complete culture medium (CCM) contains α-MEM, 1% penicillin/streptomycin and 10% FBS. All cell culture was carried out in a standard incubator with 5% CO_2 under 37°C.

The medium was changed every two days. The cells were harvested for experiments when 70% to 80 % confluence was reached. hMSCs from passage 5 to 7 were used in all experiments.

2.5. Preparation of hMSC-microdevice complexes

hMSC-microdevice complexes containing 10 μm-diameter microdevices were prepared by the following procedure. A PDMS slab (0.3 cm thick) with a circular through hole (1 cm in diameter) was placed on a PNIPAM-coated glass slide to form a chamber which enclosed the printed microdevices. The chamber and slide were warmed to 37 °C in a standard incubator. A pre-warmed (37 °C) suspension of single hMSCs in 200 μL culture medium was added to the chamber and incubated for 45 min in a standard incubator as shown in Fig. 1. The temperature of the chamber was lowered to 20 °C and the suspension was transferred to a 1.5 mL centrifuge tube and centrifuged at 60 g for 10 min to remove unbound microdevices in the supernatant. The pellet was re-suspended in 200 μL medium for further experiment.

hMSC-microdevice complexes containing 7 μm-diameter microdevices were prepared by the following procedure. A PDMS slab (0.5 cm thick) with a circular through hole (0.7 cm in diameter) was placed on an array of 7 μm-diameter microdevices printed on a PNIPAM film covering the floor of a well of a 12-well plate to form a chamber which enclosed approximately 96,000 microdevices. The chamber and slide were warmed to 37 °C in a standard incubator. A pre-warmed (37 °C) suspension of approximately 10,000 single hMSCs in 150 μL culture medium was added to the chamber and incubated for 45 min in a standard incubator as shown in Fig. 1. The temperature of the chamber was lowered to 20 °C and the suspension was transferred to a 1.5 mL centrifuge tube and centrifuged at 100 g for 5 min to remove unbound microdevices in the supernatant. The pellet was re-suspended in medium for further experiments.

hMSC-microdevice complexes composed of two different types of microdevices were prepared by sequentially attaching two types of microdevices to the same population of hMSCs. The procedure for attaching each type of microdevices was the same as above.

2.6. Stability of hMSC-microdevice complexes

The hMSC-microdevice complexes were seeded in a 96-well tissue culture plate at a density of 1,500 cell/cm^2. Medium was changed after 3 h to remove unattached cells. Medium was removed after 12 h of incubation and cells were treated with 0.25% trypsin-EDTA at 37 °C for 10 min followed by centrifugation at 60 g for 10 min to remove detached microdevices. Numbers of cell-microdevices complexes were determined by manually counting at before seeding, *i.e.*, 0 h and after trypsin treatment.

2.7. MTT assay

The samples were incubated with an MTT solution (0.5 mg/mL) in culture medium at 37˚C for 45 min. After aspiration and washing with phosphate-buffered saline (PBS), dimethyl sulfoxide was added for colorimetric measurement. Absorbance was measured by a microplate reader

(Bio-Rad Laboratories, Hercules, CA) at a wavelength of 570 nm with background subtraction at 660 nm.

2.8. PicoGreen assay

hMSC-microdevice complexes containing 7 μm-diameter microdevices were used in this assay. Briefly, proteinase K was added to the samples and incubated at 50 °C for overnight to lyse the cells [18]. PicoGreen was then added to the samples to stain the DNA. Fluorescence intensities of the samples were measured with a Synergy HTX multi-mode microplate Reader (BioTek, Winooski, VT) and used to calculate amounts of DNA and numbers of cells by assuming that a cell contained 7 pg DNA on average.

2.9. F-actin immunostaining

Alexa Fluor™ 594 phalloidin was dissolved in methanol to reach a concentration of 6.6 μM as the stock solution. The microdevice-bound hMSCs replated on a glass coverslip were washed with PBS, fixed with 4% paraformaldehyde for 15 min, permeabilized with 0.5% Triton X-100 for 5 min. hMSCs were then incubated with a 1:40 dilution of the stock solution in the dark at room temperature for 30 min. The samples were gently washed with PBS for three times before imaging.

2.10. Migration assay

A rectangular PDMS stab (10 mm × 30 mm) was placed at the center of a well of a 96-well plate. A mixture of 75% of microdevice-bound hMSCs and 25% of bare hMSCs in the CCM was seeded in the well and kept in an incubator at 37˚C. 24 h later, the slab was removed. The cells were then stained and imaged at different time points. The number of cells migrated into the detection zone was analyzed with ImageJ (National Institutes of Health, https://imagej.nih.gov/ij/).

2.11. Formation of hMSC spheroids and cell dissociation from spheroids

To form a hMSC spheroid, a mixture of microdevice-bound hMSCs and bare hMSCs with a total number of about 3,000 in the CCM were added in a well of an ultra-low attachment 96-well plate (Corning, Corning, New York) with a round bottom, and cultured in the standard incubator for 2 days. To allow cell dissociation from the spheroids, the spheroids were replated in a well of a regular 96-well tissue culture plate and kept in the standard incubator for up to 6 days.

2.12. Characterization

Optical micrographs were obtained using an inverted Nikon Ti epifluorescence microscope equipped with an Andor iXonEM+ 885 EMCCD camera. Atomic force microscopy (AFM) images were obtained using a Bruker Dimension Icon atomic force microscope operated in the tapping mode in air.

2.13. Statistical analysis

Data are expressed as mean ± standard deviation. Each experiment was triplicated. Student's t-test was performed to evaluate difference of the data, except for that in Fig. 5G, one-way ANOVA was performed to evaluate difference of multiple data sets. The differences were regarded as significant at *p <0.05 and very significant at **p <0.01. NS stands for not significant.

3. Results and discussion

The microdevices were characterized with atomic force microscopy (AFM) and optical microscopy. **Figs. 2A and 2B** are representative AFM images of PAH/PSS/PAH and PAH/PSS/PAH/PPMA microdevices respectively. These images showed that both the PAH/PSS/PAH tri-layer and the PAH/PSS/PAH/PPMA multilayer were uniform in thickness over an individual microdevice. Moreover, the microdevices had a diameter of 10 μm, which was equal to the diameter of the micropillars of the stamp. Most importantly, the AFM measurement revealed that the thickness of the PAH/PSS/PAH microdevices was roughly 6 nm and that of the PAH/PSS/PAH/PPMA microdevices was about 70 nm (**Fig. 2C**), indicating that the thickness of PPMA layer was about 64 nm. To confirm that the microdevices actually contained all layers as designed, PLL-FITC/HSA/PLL/PLGA(R18) microdevices, where PLL-FITC represents PLL chemically conjugated with FITC and PLGA(R18) is PLGA mixed with R18 dye, were fabricated. As shown in **Fig. 2D,** both PLL-FITC and PLGA(R18) layers, which were two outermost layers of the microdevices, were observed in the microdevices as evidenced by the overlapped green (FITC) and red (R18) fluorescence. This result indicated that the microdevices indeed had a composition of PLL-FITC/HSA/PLL/PLGA(R18). The highly ordered array in **Fig. 2D** was typically obtained over the entire printing area (1×1 cm^2). Moreover, since PLL is a polypeptide, HSA is a natural human protein, and PLGA is a biodegradable polymer being clinically used for drug delivery in human, the PLL-FITC/HSA/PLL/PLGA(R18) microdevices are likely to be biocompatible and biodegradable as their component materials.

The hMSC-microdevice complexes were produced by seeding hMSCs on the PAH/PSS/PAH/PPMA(R18) microdevices printed on a PNIPAM sacrificial layer and then dissolving the PNIPAM layer. It is of note that the top layer of the microdevices on the PNIPAM-coated glass slide was made of PAH. After removing free microdevices by centrifugation, a suspension of hMSC-microdevice complexes was obtained as shown in **Fig. 2E**. A complex typically consisted of a cell and a microdevice is shown in the inset of the figure, which also clearly reveals that the microdevice was attached to the outer surface of the hMSC. We believe that the electrostatic attraction between the outermost PAH layer of the microdevices and sialic acid groups on the cell surface was responsible for the bonding force between the microdevices and the hMSCs. Note that PAH was used to construct the cell-adhesive layer of microdevices in a previous study of our group [9].

This method for producing the hMSC-microdevice complexes allows an easy control of percentage of the complexes among all cells and absolute number of the complexes by adjusting the number ratio between the seeded cells and the printed microdevices as shown in **Fig. 2F**. At a cell-to-microdevice ratio of 0.1:1, about 75% of cells were bound by microdevices. In contrast, at a cell-to-microdevice ratio of 0.5:1, only 58% of cells were bound by microdevices. The higher complex percentage was accompanied by a lower absolute number of the complexes because a fixed number of microdevices was used every time for preparing the complexes. As a result, a low cell-to-microdevice ratio should be used when a high percentage of the complexes is desired and a high cell-to-microdevice ratio should be used when a high absolute number of the complexes is the target.

The method in **Fig. 1** can be easily extended to produce hMSC-microdevice complexes composed of a hMSC and two different types of microdevices by sequentially seeding the cells onto the different microdevices (**Fig. 2G**). A suspension of such complexes is shown in **Fig. 2H.** Since the different types of microdevices can, in principle, carry different drugs, this system potentially allows a versatile and synergistic delivery of multiple drugs.

Undifferentiated hMSCs can adhere to a solid surface and exhibit a spindle-like shape [19]. To evaluate whether this property of hMSCs was affected by the microdevice attachment, we seeded suspended hMSC-microdevice complexes on a regular cell-culture surface. The complexes adhered to the surface and the cells in the complexes became elongated in 12 h as shown in **Fig. 3A**. It is also known that F-actin stress fibers of undifferentiated hMSCs adhered on a solid surface generally align in parallel to its long axis [19]. This arrangement of the F-actin fibers of a microdevice-bound hMSCs was not affected by the microdevice as shown in **Fig. 3B**. To quantitatively evaluate the effect of the microdevice attachment on metabolic activity the hMSCs, we performed MTT assay on a mixture of bare hMSCs (25%) and microdevice-bound hMSCs (75%) for up to 5 days with the use of pure hMSCs as a control [20,21]. The result (**Fig. 3C**) shows no significant effect of the microdevice attachment on hMSC metabolic activity at all time points of measurement. To assess the effect of microdevice attachment on proliferation of the hMSCs, we performed PicoGreen assay on a mixture of bare hMSCs (22%) and microdevice-bound hMSCs (78%) and used pure hMSCs as a control. The result (**Fig. 3D**) shows that microdevice attachment had no significant effect on hMSC proliferation at day 3 and 5 during the cultivation.

We envisioned that the microdevice-bound hMSCs might need to undergo *in vitro* cultivation before their *in vivo* use. To study whether the hMSC-microdevice complexes had enough stability to withstand the procedure, we had cultured the complexes for 12 h and then trypsinized them. The result (**Fig. 3E**) reveals that a significant fraction of the complexes remained intact. Quantitatively, when the initial complex concentration was 60% at the time of cell seeding, about 30% of the total cells were still associated with microdevices after trypsinization (**Fig. 3F**), meaning that approximately 50% of the complexes survived the 12 h-cultivation and subsequent trypsinization. Given the fact that trypsin was highly effective in detaching hMSCs from a

tissue-culture surface, our result indicates that the hMSC-microdevice complexes were relatively stable.

It is well known that systemically administered hMSCs can accumulate at injured tissues and tumors [22]. This homing ability of the hMSCs is highly attractive for cell-mediated drug delivery. While "cellular backpacks"-bound monocytes/macrophages and nanoparticles-bound hMSCs could migrate *in vitro* and *in vivo* [3,4,13], it is unknow whether the microdevice-bound hMSCs retained this ability. To partially answer this question, we performed a stopper-based assay to determine if the migratory ability of the hMSCs is affected by the microdevice attachment [23]. The assay was performed on a mixture of 75% microdevice-bound hMSCs and 25% bare hMSCs and a control, which was a pure population of bare hMSCs. The result shows that a large number of cells migrated into the detection zones in both samples (**Figs. 4A and 4B**). Some of the migrated hMSCs in the sample were microdevice-bound hMSCs (**Figs. 4C and 4D**). Moreover, there was no statistically significant difference in the number of migrated cells between the two samples (**Fig. 4E**). However, microdevice-bound hMSCs accounted for only 11.6% of all migrated hMSCs in the sample containing the complexes, suggesting that the migratory ability of hMSCs was hampered by the microdevice attachment but was retained to a significant extent. While the mechanism is unknown, we speculate that size of the microdevice might have played a key role in inhibiting the migration of the microdevice-bound hMSCs. Since the microdevices can be fabricated with a wide size range, this microdevice-based platform may offer a new strategy to control migration of the implanted hMSCs *in vivo*.

Under an appropriate condition, cultured hMSCs can self-assemble into a spherical multicellular aggregate termed as three-dimensional (3D) spheroid. Compared to the traditional two-dimensional (2D) cell culture, the spheroid-based culture improves therapeutic potential of hMSCs in various aspects, including secretion of anti-inflammatory cytokines, multi-lineage differentiation, expression of migratory cytokine receptor, secretion of trophic factors, and resistance against ischemic condition [24,25,26,27,28]. Moreover, it has been demonstrated that spheroids of rat and human MSCs outperformed single MSCs for treating nerve and kidney injuries in animal models [29,30,31]. It is thus interesting to study whether the microdevice attachment would affect the ability of the hMSCs to form a spheroid.

We added a constant total number of microdevice-bound hMSCs and bare hMSCs with a series of percentages of microdevice-bound hMSCs (0, 5, 10, 25, 50, and 75%) into an ultra-low attachment 96-well plate. The sample containing 0% microdevice-bound hMSCs served as a control. A single spheroid formed in each well (**Figs. 5A-5F**). All spheroids except the control showed fluorescence of R18 and the fluorescence intensity increased with the increase of the percentage of the microdevice-bound hMSCs. This result indicates that the microdevice-bound hMSCs were incorporated into the spheroids as the control hMSCs. In other words, the microdevice attachment did not affect the ability of hMSCs to form a 3D spheroid.

The spheroids consisting of different percentages of microdevice-bound hMSCs had roughly the same size (**Fig. 5G**). This can be explained as follows. The volume of a single microdevice

(diameter = 10 μm and thickness = 0.07 μm) is about 5.5 μm^3. It has been reported that hMSCs in a spheroid have an average diameter of 11-12 μm and average volume between 779 - 985 μm^3 depending on the size of the spheroid [24]. Assuming that 75% hMSCs in a spheroid were bound by a microdevice, the microdevices would only occupy at most 0.7% of the volume of an organoid. Since this volume percentage decreased proportionally as the percentage of microdevice-bound hMSCs in a spheroid decreased, the presence of the microdevices in a hMSC spheroid therefore did not significantly affect the diameter of the spheroid.

Dissociation of hMSCs from a spheroid is sometimes essential for its therapeutic application [31]. We thus studied whether the microdevice-bound hMSCs in a spheroid retained this ability by replating spheroids prepared from 0% and 50% microdevice-bound hMSCs respectively in a regular tissue-culture plate. We observed that cells dissociated from the spheroids as shown in (**Figs. 5H and 5I**). Based on the number and travel distance of the dissociated cells, the overall dissociation abilities of the two spheroids were comparable. Many dissociated hMSCs were colocalized with the microdevices in the microdevice-containing sample (**Fig. 5I**), suggesting that they were microdevice-bound hMSCs. However, the percentage of the dissociated microdevice-bound hMSCs was significantly lower than the initial percentage of the microdevice-bound hMSCs for forming the spheroid. This could be attributed to the proliferation of the cells during the 6-day culture after replating the spheroids and/or the reduced migratory ability of the microdevice-bound hMSCs as observed in the stopper-based migration assay. It is worth noting that some microdevice-bound hMSCs migrated over a much longer distance than most dissociated bare hMSCs, as exemplified by the two microdevice-bound hMSCs 2.5 mm away from the spheroid in (**Fig. 5K**). The above result indicates that the microdevice-bound hMSCs in a spheroid were able to dissociate from a spheroid, but a quantitative measurement of the effect of microdevice attachment on the dissociation ability and the mechanism awaits a further study.

Although the tumoritropic capability of our microdevice-based hMSC-mediated drug delivery system has not been fully validated, it is worthwhile to note that the microdevices can be engineered to carry multiple classes of therapeutic agents for treating solid tumors. Specifically, we previously loaded a drug-like small molecule into the PLGA layer of the microdevices [6]. The same method can be used to load small-molecule hydrophobic chemotherapeutics such as doxorubicin and paclitaxel into the microdevices. We also incorporated a proteinaceous enzyme into the microdevices through LbL assembly [7], indicating that antitumor enzymes such as carboxypeptidase and kynureninase can be loaded in the microdevices [32,33]. Moreover, we and coworkers created microdevices containing radiosensitizing nanoparticles and demonstrated the microdevices were able to enhance X-ray radiation killing of cancer cells [34]. With a potential to further enhance the accumulation of the above classes of therapeutic agents in the solid tumors, our microdevice-based hMSC-mediated drug delivery system promises to significantly improve these therapies for treating solid tumors.

4. Conclusion

In this study, we developed a novel microdevice-based hMSC-mediated drug delivery system. The microdevices could be attached to the hMSCs in a versatile, well-controlled manner. The hMSC-microdevice complexes produced in this study were relatively stable over cultivation and trypsinization. The microdevice attachment did not affect the viability and proliferation of the hMSCs. Moreover, the microdevice-bound hMSCs retained their abilities to migrate on a 2D surface, form a 3D spheroid, and actively dissociate from the spheroid. These results indicate that this system holds potential to be further developed into a clinically viable cell-mediated drug delivery system.

Acknowledgment

This study was supported by National Science Foundation award 1547730.

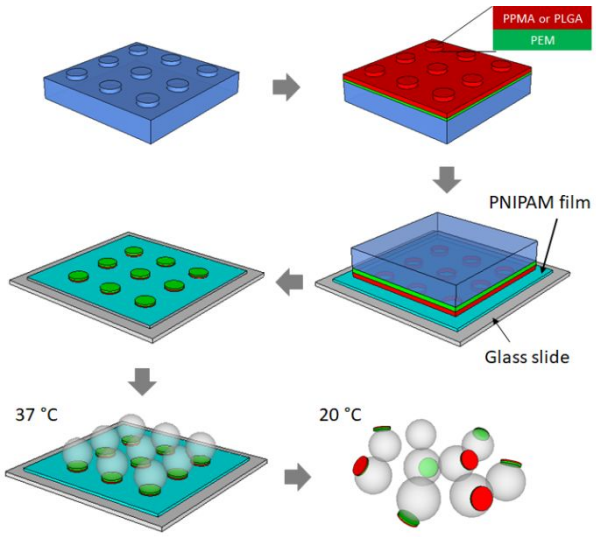

Fig. 1. Procedure for producing hMSC-microdevice complexes. PEM: polyelectrolyte multilayer.

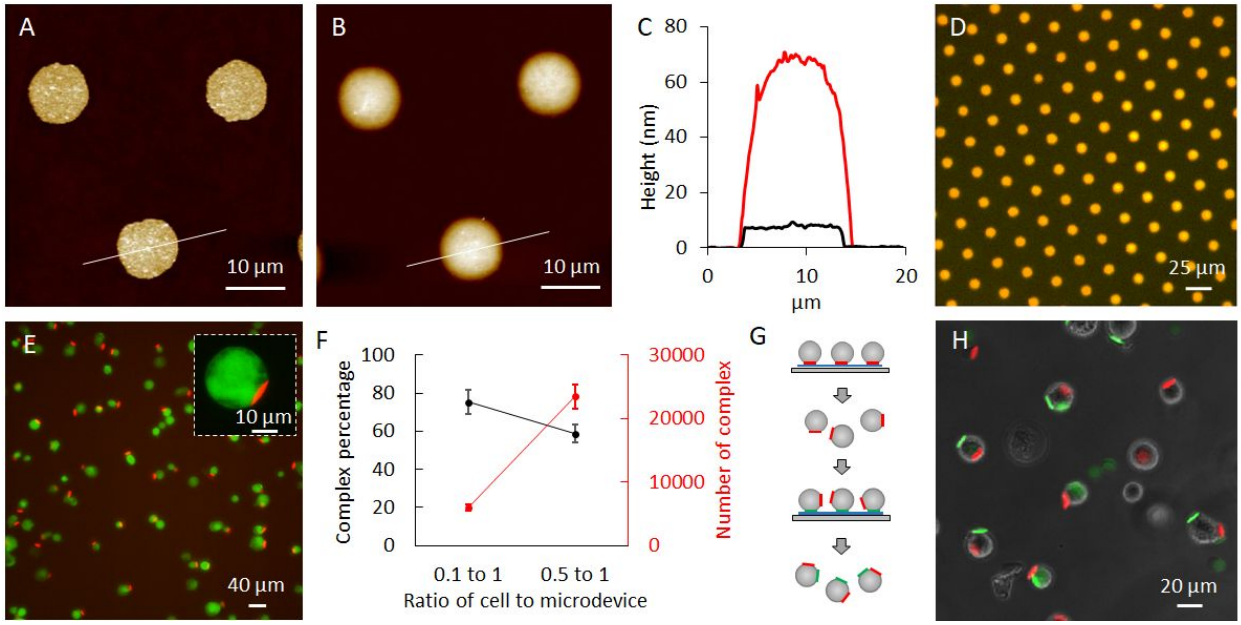

Fig. 2. Characterization of microdevices and hMSC-microdevice complexes. Height AFM images of (A) PAH/PSS/PAH and (B) PPMA/PAH/PSS/PAH microdevices printed on a glass slide. (C) Height profiles along the white lines in (A) and (B). Black curve represents for (A) and red curve represents for (B). (D) Fluorescence image of an array of PLL-FITC/HSA/PLL/PLGA(R18) microdevices on a PNIPAM-coated glass slide generated by superimposing a green fluorescence image for FITC and a red fluorescence image for R18. (E) Fluorescence image of suspended hMSC-microdevice complexes. Inset shows a magnified complex. hMSCs were stained with calcein AM (green). Microdevices had a composition of PAH/PSS/PAH/PPMA(R18) (red). (F) Effects of number ratio between seeding cells to the microdevices on the percentage and absolute number of the complexes. (G) Scheme of producing hMSC-microdevice complexes composed of a hMSC and two different types of microdevices (red and green). (H) Fluorescence image of hMSC-microdevice complexes prepared by the procedure in (G). The two types of microdevices were PAH/PSS/PAH/PPMA(R18) (red) and PAH/PSS/PAH/PPMA(DiO) (green) respectively.

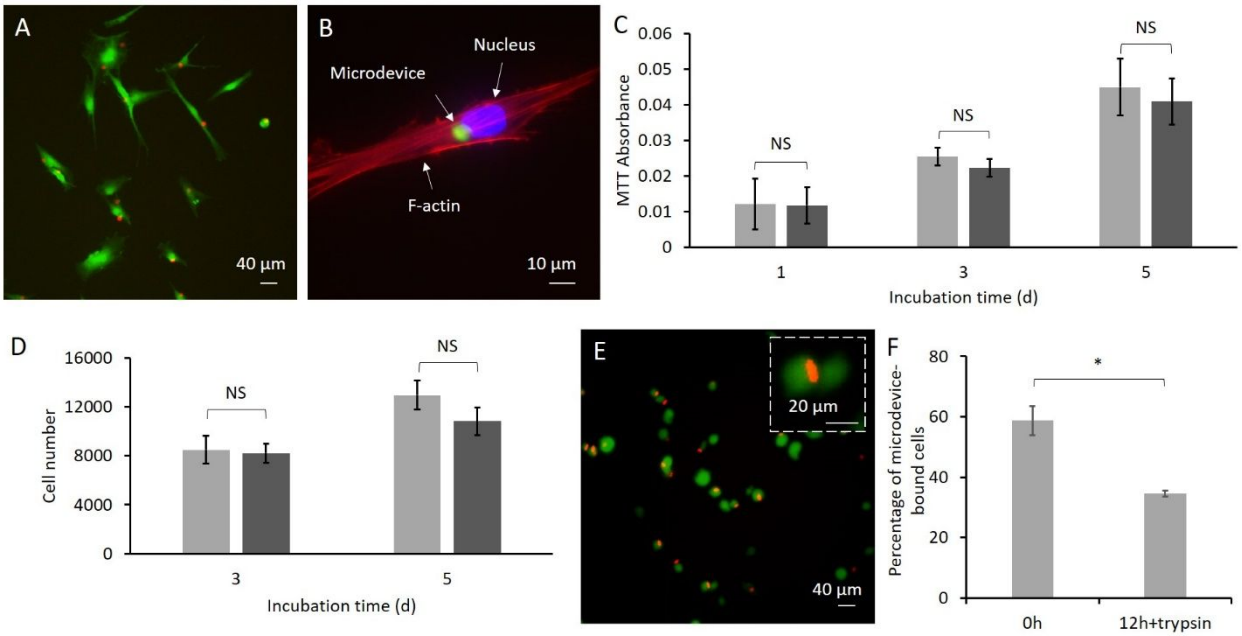

Fig. 3. Effects of microdevice attachment on cellular properties and stability of the hMSC-microdevice complexes. (A) Fluorescence image of hMSC-microdevice complexes seeded on a cell-culture surface and cultured for 12 h. hMSCs were stained with calcein AM (green). Microdevices had a composition of PAH/PSS/PAH/PPMA(R18) (red). (B) Immunostaining of F-actin (red) of a hMSC-microdevice complexes seeded on a cell-culture surface and cultured for 12 h. The microdevice had a composition of PAH/PSS/PAH/PPMA(DiO) (green) and the cell nucleus was stained with Hoechst 33342 (blue). (C) MTT assay result of a mixture of microdevice-bound hMSCs (75%) and bare hMSCs (25%, light bars) and hMSCs (100%, dark bars). (D) PicoGreen assay result of a mixture of microdevice-bound hMSCs (78%) and bare hMSCs (22%, light bars) and hMSCs (100%, dark bars). (E) Fluorescence image of hMSC-microdevice complexes firstly seeded on a cell-culture surface and cultured for 12 h and then trypsinized. hMSCs were stained with calcein AM (green). Microdevices had a composition of PAH/PSS/PAH/PPMA(R18) (red). (F) Percentages of complexes before seeding and after 12 h-cultivation and trypsinization. NS denotes not significant. * indicates $p < 0.05$.

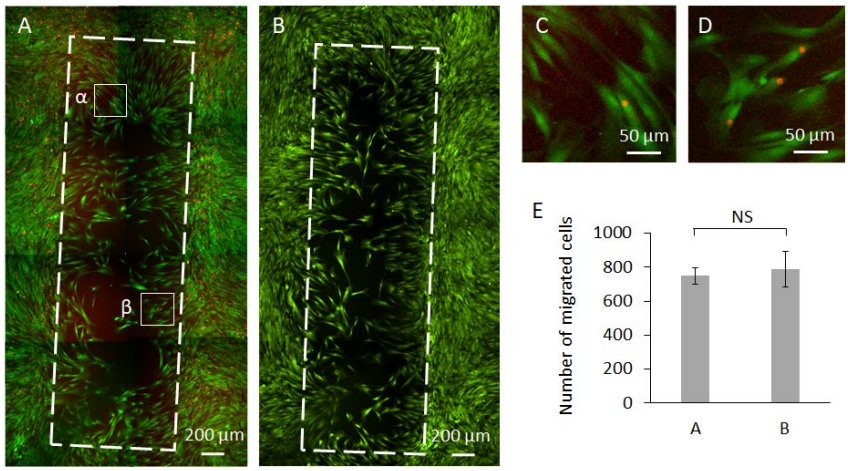

Fig. 4. Effect of microdevice attachment on hMSC migration. Fluorescence images of (A) mixed microdevice-bound hMSCs and bare hMSCs and (B) bare hMSCs 24 h after removing the stoppers, (C) magnified area enclosed by the square marked by α in (A), and (D) magnified area enclosed by the square marked by β in (A). (E) Comparison between numbers of the migrated cells in (A) and (B). The detection zones are areas enclosed by white dashed rectangles in (A) and (B). Cells were stained with calcein AM (green) and the microdevices had a composition of PAH/PSS/PAH/PPMA(R18) (red). NS denotes not significant.

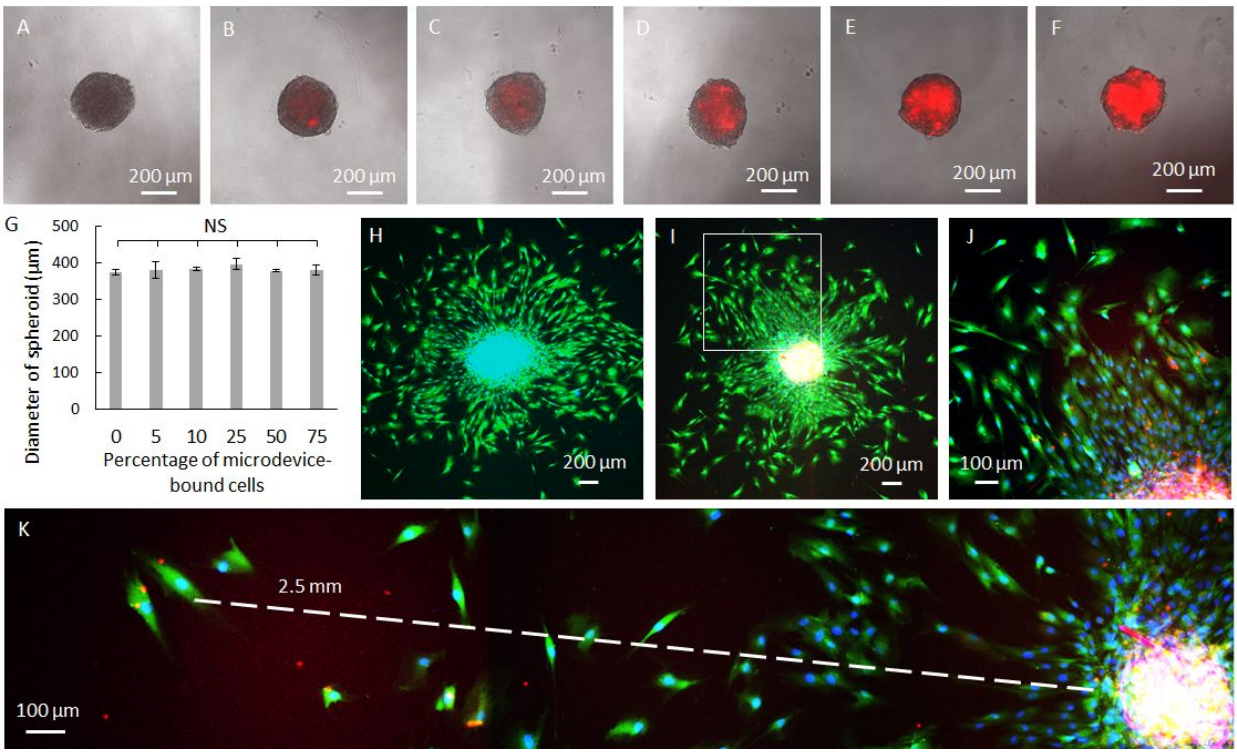

Fig. 5. Effect of microdevice attachment on the formation of a hMSC spheroid and cell dissociation from a spheroid. Merged fluorescence and phase-contrast micrographs of spheroids formed from hMSCs with 0% (A), 5% (B), 10% (C), 25% (D) 50% (E), and 75% (F) of microdevice-bound hMSCs. (G) Statistical analysis of diameters of the spheroids formed from bare hMSCs and microdevice-bound hMSCs in (A-F). NS denotes not significant. Fluorescence images of spheroids containing 0% (H) and 50% (I) microdevice-bound hMSCs replated in a regular cell-culture plate well. (J) Magnified area enclosed by the white square in (I). (K) The spheroid in (I) and microdevice-bound and bare hMSCs dissociated from the spheroid. The microdevices were labelled with R18 (red) in (A-F, H-K). hMSCs were labeled with calcein AM and Hoechst 33342 (blue) in (H-K).

References

[1] E.V. Batrakova, H.E. Gendelman, A.V. Kabanov, Cell-mediated drug delivery, Expert Opin. Drug Deliv. 8 (2011) 415-433.

[2] Y. Su, Z. Xie, G.B. Kim, C. Dong, J. Yang, Design Strategies and Applications of Circulating Cell-Mediated Drug Delivery Systems, ACS Biomater. Sci. Eng. 1 (2015) 201-217.

[3] A.J. Swiston, C. Cheng, S.H. Um, D.J. Irvine, R.E. Cohen, M.F. Rubner, Surface Functionalization of Living Cells with Multilayer Patches, Nano Lett. 8 (2008) 4446-4453.

[4] N.L. Klyachko, R. Polak, M.J. Haney, Y. Zhao, R.J.G. Neto, M.C. Hill, A.V. Kabanov, R.E. Cohen, M.F. Rubner, E.V. Batrakova, Macrophages with cellular backpacks for targeted drug delivery to the brain, Biomaterials 140 (2017) 79-87.

[5] P. Zhang, J. Guan, Fabrication of multilayered microparticles by integrating layer-by-layer assembly and microcontact printing, Small 7 (2011) 2998–3004.

[6] J. Xia, Z. Wang, D. Huang, Y. Yan, Y. Li, J. Guan, Asymmetric biodegradable microdevices for cell-borne drug delivery, ACS Appl. Mater. Interfaces 7 (2015) 6293-6299.

[7] J. Xia, Z. Wang, Y. Yan, Z. Cheng, L. Sun, Y. Li, Y. Ren, J. Guan, Catalase-laden microdevices for cell-mediated enzyme delivery, Langmuir 32 (2016) 13386-13393.

[8] Z. Wang, J. Xia, P. Hoang, L. Sun, S. Luo, Z. Cheng, Y. Ren, T. Liu, J. Guan, Fabrication of carbon nanotube-laden microdevices for Raman labeling of macrophages, Biomed. Phys. Eng. Express 3 (2017) 025012.

[9] Z. Wang, J. Xia, Y. Yan, A.C. Tsai, Y. Li, T. Ma, J. Guan, Facile functionalization and assembly of live cells with microcontact-printed polymeric biomaterials, Acta Biomater. 11 (2015) 80-87.

[10] D.J. Prockop, D.J. Kota, N. Bazhanov, R.L. Reger, Evolving paradigms for repair of tissues by adult stem/progenitor cells (MSCs), J. Cell Mol. Med. 14 (2010) 2190-2199.

[11] D.F. Stroncek, M. Sabatino, J. Ren, L. England, S.A. Kuznetsov, H.G. Klein, P.G. Robey, Establishing a bone marrow stromal cell transplant program at the National Institutes of Health Clinical Center, Tissue Eng. Part B Rev. 20 (2014) 200-205.

[12] M.R. Reagan, D.L. Kaplan, Concise review: mesenchymal stem cell tumor-homing: detection methods in disease model systems, Stem cells 29 (2011) 920-927.

[13] H. Cheng, C.J. Kastrup, R. Ramanathan, D.J. Siegwart, M. Ma, S.R. Bogatyrev, Q.B. Xu, K.A. Whitehead, R. Langer, D.G. Anderson, Nanoparticulate cellular patches for cell-mediated tumoritropic delivery, ACS Nano. 4 (2010) 625-631.

[14] M. Roger, A. Clavreul, M.C. Venier-Julienne, C. Passirani, L. Sindji, P. Schiller, C. Montero-Menei, P. Menei, Mesenchymal stem cells as cellular vehicles for delivery of nanoparticles to brain tumors, Biomaterials 31 (2010) 8393-8401.

[15] L.L. Li, Y.Q. Guan, H.Y. Liu, N.J. Hao, T.L. Liu, X.W. Meng, C.H. Fu, Y.Z. Li, Q.L. Qu, Y.G. Zhang, S.Y. Ji, L. Chen, D. Chen, F.Q. Tang, Silica nanorattle-doxorubicin-anchored mesenchymal stem cells for tumor-tropic therapy, ACS Nano. 5 (2011) 7462-7470.

[16] T. Sadhukha, T.D. O'Brien, S. Prabha, Nano-engineered mesenchymal stem cells as targeted therapeutic carriers, J. Control. Release 196 (2014) 243-251.

[17] A.C. Tsai, Y.J. Liu, X.G. Yuan, T. Ma, Compaction, fusion, and functional activation of three-dimensional human mesenchymal stem cell aggregate, Tissue Eng. Part A 21 (2015) 1705-1719.

[18] J. Kim, T. Ma, Bioreactor strategy in bone tissue engineering: Pre-culture and osteogenic differentiation under two flow configurations. Tissue Eng. Part A 18 (2012) 2354-2364.

[19] G. Yourek, M.A. Hussain, J.J. Mao, Cytoskeletal changes of mesenchymal stem cells during differentiation, ASAIO J. 53 (2007) 219–228.

[20] C.W. Lu, J.K. Hsiao, H.M. Liu, C.H. Wu, Characterization of an iron oxide nanoparticle labelling and MRI-based protocol for inducing human mesenchymal stem cells into neural-like cells, Sci. Rep. 7 (2017) 3587.

[21] E. Lucarelli, A. Beccheroni, D. Donati, L. Sangiorgi, A. Cenacchi, A.M.D. Vento, C. Meotti, A.Z. Bertoja, R. Giardino, P.M. Fornasari, M. Mercuri, P. Picci, Platelet-derived growth factors enhance proliferation of human stromal stem cells, Biomaterials 24 (2003) 3095-3100.

[22] G. Chamberlain, J. Fox, B. Ashton, J. Middleton, Concise review: mesenchymal stem cells: their phenotype, differentiation capacity, immunological features, and potential for homing, Stem Cells 25 (2007) 2739-2749.

[23] K.P. Goetsch, C.U. Niesler, Optimization of the scratch assay for in vitro skeletal muscle wound healing analysis, Anal. Biochem. 411 (2011) 158-160.

[24] T.J. Bartosh, J.H. Ylöstalo, A. Mohammadipoor, N. Bazhanov, K. Coble, K. Claypool, R.H. Lee, H. Choi, D.J. Prockop, Aggregation of human mesenchymal stromal cells (MSCs) into 3D spheroids enhances their antiinflammatory properties, Proc. Natl. Acad. Sci. U. S. A. 107 (2010) 13724-13729.

[25] I.A. Potapova, P.R. Brink, I.S. Cohen, S.V. Doronin, Culturing of human mesenchymal stem cells as three-dimensional aggregates induces functional expression of CXCR4 that regulates adhesion to endothelial cells, J. Biol. Chem. 283 (2008) 13100-13107.

[26] S. Sart, A.C. Tsai, Y. Li, T. Ma, Three-dimensional aggregates of mesenchymal stem cells: cellular mechanisms, biological properties, and applications, Tissue Eng. Part B Rev. 20 (2014) 365-380.

[27] J.A. Zimmermann, T.C. McDevitt, Pre-conditioning mesenchymal stromal cell spheroids for immunomodulatory paracrine factor secretion, Cytotherapy 16 (2014) 331-345.

[28] T.J. Bartosh, J.H. Ylöstalo, N. Bazhanov, J. Kuhlman, D.J. Prockop, Dynamic compaction of human mesenchymal stem/precursor cells into spheres self-activates caspase-dependent IL1 signaling to enhance secretion of modulators of inflammation and immunity (PGE2, TSG6, and STC1), Stem Cells 31 (2013) 2443-2456.

[29] Y. Xu, T.P. Shi, A. Xu, L. Zhang, 3D spheroid culture enhances survival and therapeutic capacities of MSCs injected into ischemic kidney, J Cell Mol. Med. 20 (2016) 1203-1213.

[30] E.J. Lee, L.J. Xu, G.H. Kim, S.K. Kang, S.W. Lee, S.H. Park, S. Kim, T.H. Choi, H.S. Kim, Regeneration of peripheral nerves by transplanted sphere of human mesenchymal stem cells derived from embryonic stem cells, Biomaterials 33 (2012) 7039-7046.

[31] T.C. Tseng, S.H. Hsu, Substrate-mediated nanoparticle/gene delivery to MSC spheroids and their applications in peripheral nerve regeneration, Biomaterials 35 (2014) 2630-2641.

[32] S.K. Sharma, K.D. Bagshawe, Antibody directed enzyme prodrug therapy (ADEPT): trials and tribulations, Adv. Drug Deliv. Rev. 118 (2017) 2-7.

[33] T.A. Triplett, K.C. Garrison, N. Marshall, M. Donkor, J. Blazeck, C. Lamb, A. Qerqez, J.D. Dekker, Y. Tanno, W.C. Lu, C.S. Karamitros, K. Ford, B. Tan, X.M. Zhang, K. McGovern, S. Coma, Y. Kumada, M.S. Yamany, E. Sentandreu, G. Fromm, S. Tiziani, T.H. Schreiber, M. Manfredi, L.I.R. Ehrlich, E. Stone, G. Georgiou, Reversal of indoleamine 2,3-dioxygenase-mediated cancer immune suppression by systemic kynurenine depletion with a therapeutic enzyme, Nat. Biotechnol. 36 (2018) 758-764.

[34] P. Zhang, Y. Qiao, J. Xia, J. Guan, L. Ma, M. Su, Enhanced radiation therapy with multilayer microdisks containing radiosensitizing gold nanoparticles, ACS Appl. Mater. Interfaces. (2015) 4518-4524.

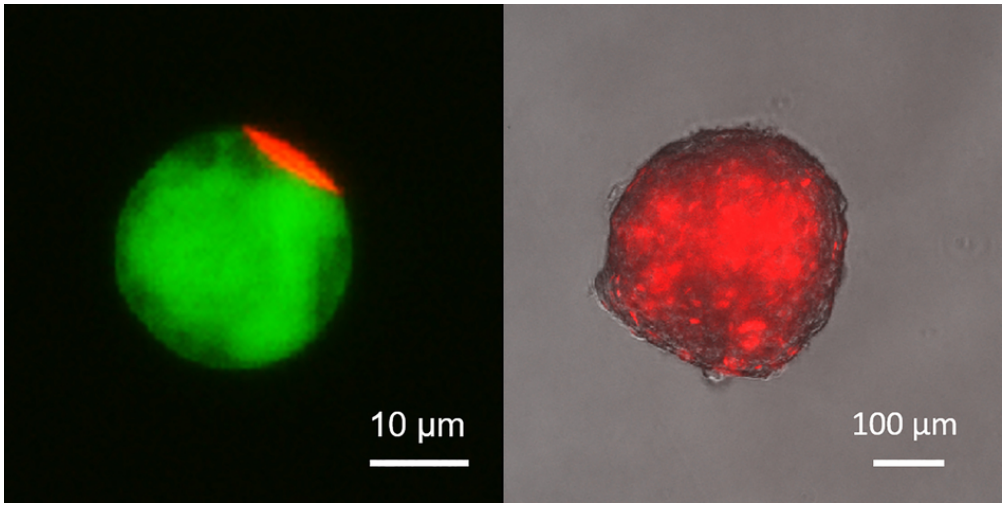

Attachment of microfabricated devices to human mesenchymal stem cells promises to enhance drug delivery to solid tumors.

79x39mm (300 x 300 DPI)